Geochemical Journal, Vol. 40, pp. 557 to 568, 2006

Lead enrichment in Neotethyan volcanic rocks from Iran: The implications of a descending slab

MOHAMMAD REZA GHORBANI*

Department of Geology, Tarbiat Modares University, Tehran 14115-175, Iran

(*Received May 30, 2005; Accepted May 31, 2006*)

Basic-intermediate volcanic rocks from the Karaj-Danesfahan area in the Neotethyan magmatic belt of Iran show typical island arc geochemical signatures. The rocks demonstrate calcalkaline affinity with low abundances of "high field strength elements" (HFSE) such as Nb, Ta, Hf and Ti, and highly distinctive spiked trace element patterns at "large ion lithophile elements" (LILE) such as Ba, K, and Sr. Comparing the geochemical characteristics of two sets of the volcanic rocks sampled from two parts of the study area 100 km apart, however, indicate subtle but significant geochemical differences which bear important petrogenetic implications. One set of the volcanic rocks is abnormally enriched in Pb and shows consistently higher abundances of HFSE, particularly Ti, than the other set. These two series are called HTL series (after high titanium and lead) and LTL series (after low titanium and lead), respectively. HTL series volcanic rocks are further from the subduction axis, so they should have had a deeper descending slab contributing to their mantle wedge magmatism. To be able to release Pb-enriched fluids, the subducting slab should not have undergone earlier dehydration. It is because Pb is highly incompatible. It appears that in the early stage, subduction proceeded at a higher rate (cold slab), so slab-dehydration occurred at greater depths triggering HTL series magmatism. Subsequently the subduction rate decreased which in turn raised isotherms and promoted partial melting at shallower depths leading to LTL series magmatism.

Keywords: island arc basalt, trace elements geochemistry, REE, Iran, Neotethys

INTRODUCTION

Volcanic rocks from the Danesfahan-Karaj area are the northernmost part of a major tectonomagmatic unit, the Urumieh-Dokhtar magmatic assemblage (UDMA; see Fig. 1), interpreted to be the product of "island arc" magmatism during subduction of the Neotethyan oceanic realm in late Mesozoic and Cenozoic time (Alavi, 1996). Berberian and Berberian (1981) considered the UDMA as "active continental margin" type magmatism, however, they reported Paleogene andesites from Natanz (also located in the UDMA; Fig. 1-a) with trace element signatures of island arcs. Controversy exists on the evolution of the Neotethyan subduction zone, its boundaries and interactions with neighbouring plates. This is mainly due to a severe shortage of diagnostic geochemical data and petrological studies on volcanic rocks from this tectonomagmatic unit, the UDMA. Such data would help draw a better picture of the make up of this important, yet poorly understood magmatic belt of our planet extending almost 2000 km from northwest to southern Iran.

The basic-intermediate volcanic rocks being studied are part of a thick volcanosedimentary sequence referred to as the Karaj Formation (i.e., 3.3 km thickness in its type-section) that embrace the whole Eocene time span. The Karaj Formation was formally introduced by Dedual (1967) and its details can be found in Stocklin and Setudehnia (1971). Volcanic rocks dominate the middle part of the formation. At lower levels they are mainly of basic compositions that grade into intermediate and felsic varieties upwards. These basic to felsic volcanic rocks collectively form consistent curvilinear arrays on Harker variation diagrams (see Appendix), thereby confirming the role of fractional crystallization in their evolution. Index fossils reported from numerous lenticular bodies of calcareous tuffs and numulitic limstones found embedded in the middle part of the sequence confirm the Middle Eocene age for the volcanics being studied (Eghlimi *et al.*, 1999; Mehdizadeh-Tehrani *et al.*, 1995).

Danesfahan-Karaj and adjoining areas were the subjects of a few petrological studies in the last three decades. The studies were, however, limited to major element geochemistry and only rarely were the samples analysed for Rb, Sr, and Ba. This set of analytical data is available from the author on request. A critical review of these data was utilised in selecting the study areas (south Danesfahan and south Karaj) for sampling and further

*e-mail address: ghorbani@modares.ac.ir

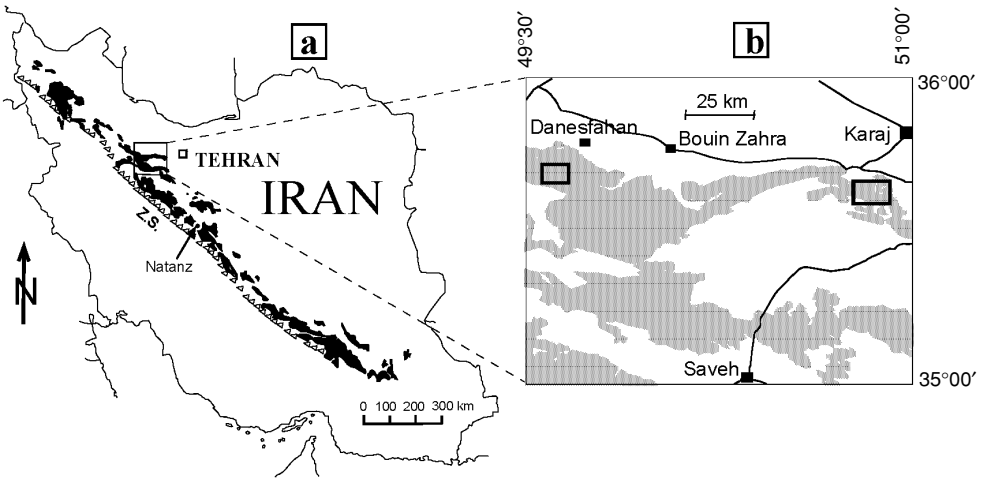

Fig. 1. (a) The Urumieh-Dokhtar magmatic assemblage (UDMA) is shown in black on a map of Iran (after Alavi, 1994). Towards the southwest, the UDMA is limited to the Zagros Suture (Z.S.). (b) Location of the study areas, S Karaj and S Danesfahan. The stippled area indicates Tertiary magmatic rocks (after Saveh Geological map of Amidi, 1984).

geochemical studies (see Appendix). In the current study, 120 samples were collected as a result of 20 days field-work in 2002. Eighty of the samples were selected for thin sectioning. Amongst the least altered samples, 14 were used for chemical analysis. This is the first account, based on a comprehensive major and trace element data set, of petrology and geochemical characteristics of the Eocene volcanic rocks from south Danesfahan and south Karaj areas, Iran (Fig. 1).

Analytical Techniques

A representative set of 14 basic-intermediate volcanic rocks from the study area was analysed for their major and trace elements for the first time (Table 1). Whole rock analyses for major elements, and the trace elements Pb, Rb, Sr, Ba, Nb, Zr, Y and Th (Table 1) were obtained by X-ray fluorescence (XRF) at the University of New South Wales, Sydney following the procedures of Norrish and Hutton (1969). The analyses were carried out on a Phillips PW2400 XRF spectrometer using 40 mm glass disks and 40 mm pressed pellets for major- and trace-element analyses, respectively. Instrumental neutron activation analysis (INAA) was employed for REE, Ta, Hf, Cr, Sc and Th analyses of the whole-rock samples at the Becquerel Laboratories, ANSTO, Sydney, using the HIFAR reactor at Lucas Heights (for the procedures used, see Gordon *et al*., 1968).

In-house standards were also analysed to check the accuracy of the methods. Table 2 includes the recommended abundances and average abundances (for three individual analyses) of trace element in the standards used. Analytical reproducibility was also examined. For those trace elements analysed by INAA, errors were evaluated to be better than 2% with the exception of Nd (4%), Ho (15%), Tb (20%) and Ta (30%). For those trace elements analysed by XRF, errors were evaluated to be better than 5% except Nb (10%). Detection limits (DL) are presented in Table 1. Duplicates run for the analyses indicate that the errors for major elements are better than 1% except alkaline elements (4%).

The whole rock analyses totals are in the range 99.02 to 100.73 with a mean of 99.62 wt.% (Table 1). Diagrams depicted and figures (e.g., Mg# value) presented are based on a major element analyses recalculation to 100%, on an anhydrous basis.

Rock Classification

On the TAS (total alkalis versus silica) diagram, volcanic rocks from the study areas fall on the boundary between subalkaline and midalkaline fields (lower diagrams in Fig. 2), however, the most basic samples are subalkaline. The calcalkaline character of the subalkaline volcanic rocks is indicated by the AFM diagram (Na_2O+K_2O-FeO_t-MgO; Fig. 3). Geochemistry of the volcanic rocks also conform to Peacock's calcalkaline character of igneous rocks (Peacock, 1931), recommended by Arculus (2003) as a useful tool. On tectonomagmatic discrimination diagrams for basaltic rocks (e.g., 2Nb-Zr/4-Y; Meschede, 1986), volcanic rocks from both series fall in the volcanic arc basalt field (not shown).

In Fig. 2 volcanic rocks are depicted on Harker diagrams. On most of these diagrams, data points from the two areas overlap. However, south Karaj volcanic rocks show distinctly higher TiO_2 and Pb than the volcanic rocks

Table 1. Major and trace element (including REE) analyses of a set of basic-intermediate volcanic rocks from S Danesfahan (DS 1–7) and S Karaj (KJ 1–7)

	S Danesfahan volcanic rocks							S Karaj volcanic rocks						
	DS1	DS2	DS3	DS4	DS5	DS6	DS7	KJ1	KJ2	KJ3	KJ4	KJ5	KJ6	KJ7
SiO_2	51.74	51.79	52.94	55.22	59.09	63.88	62.19	54.93	58.20	61.89	67.40	56.01	56.32	62.01
TiO_2	0.58	0.72	0.72	0.76	0.70	0.67	0.53	1.14	1.05	1.01	0.65	1.01	1.05	1.11
Al_2O_3	20.64	19.68	16.79	20.15	18.55	16.44	17.92	19.16	17.05	16.27	15.21	17.17	18.22	15.56
FeOt	8.48	10.11	8.68	7.81	5.05	6.05	3.70	7.87	7.43	6.51	4.53	6.41	6.54	7.22
MnO	0.14	0.13	0.14	0.12	0.11	0.16	0.15	0.11	0.27	0.14	0.10	0.55	0.52	0.13
MgO	4.49	4.52	5.96	2.58	1.78	1.59	0.47	2.69	2.12	2.11	1.02	1.69	2.66	1.47
CaO	9.00	8.44	9.42	8.17	6.59	4.49	3.63	7.57	7.57	3.85	1.46	7.84	9.37	5.36
Na_2O	3.31	4.02	2.70	3.25	3.24	3.82	4.39	3.54	3.73	3.52	3.84	2.73	3.02	3.04
K_2O	0.85	0.40	2.29	1.69	4.48	2.62	6.76	2.54	2.17	4.26	5.57	6.25	2.05	3.74
P_2O_5	0.71	0.14	0.27	0.18	0.34	0.23	0.20	0.40	0.33	0.37	0.16	0.36	0.24	0.35
SO_3	0.05	0.06	0.08	0.06	0.07	0.04	0.06	0.06	0.08	0.07	0.05	0.00	0.00	0.00
Total	100.00	100.00	100.00	100.00	100.00	100.00	100.00	100.00	100.00	100.00	100.00	100.00	100.00	100.00
L.O.I.	1.65	3.83	2.00	1.54	1.89	1.12	3.54	1.63	2.95	1.83	1.56	4.93	4.91	4.15
Mg#	0.39	0.35	0.49	0.32	0.36	0.30	0.20	0.34	0.30	0.35	0.31	0.30	0.37	0.24
Trace elements (XRF, ppm)														
Pb (2)	7.0	10.5	12.6	8.6	16.3	18.3	15.2	11.8	67.0	17.2	28.6	46.3	38.9	21.5
Rb (1)	24.7	7.4	52.2	34.6	149.6	62.9	185.8	75.1	50.5	141.5	176.5	206.4	51.2	112.8
Sr (0.9)	287.7	713.4	524.7	464.7	455.0	380.1	306.7	508.8	442.0	319.5	178.6	303.7	423.0	346.7
Ba (8)	298.0	291.8	575.0	445.8	729.5	826.8	871.9	437.2	526.5	759.1	1039.5	875.1	358.1	810.3
Nb (1)	3.1	4.5	6.3	6.7	11.3	7.6	15.8	12.0	1.5	17.9	21.7	13.3	8.1	14.4
Zr (1)	48.7	69.9	96.6	91.0	172.4	119.2	222.0	184.9	142.5	270.7	336.2	186.7	100.1	225.8
Y (1)	13.9	17.8	19.2	19.2	21.5	31.0	27.2	31.4	30.4	42.8	46.6	26.1	21.7	37.2
REE and Trace elements (NAA, ppm)														
La (0.05)	5.61	7.54	16.00	15.60	24.30	19.40	38.40	26.10	25.20	37.10	43.70	26.70	16.00	30.50
Ce (0.5)	12.20	17.00	30.50	29.50	45.60	39.10	68.80	51.00	49.30	73.80	84.90	54.20	35.40	61.30
Nd (1.0)	6.59	9.64	14.80	15.00	21.10	19.30	30.00	24.20	24.70	36.10	39.40	26.20	18.20	30.90
Sm (0.01)	1.72	2.40	3.36	3.45	4.21	4.63	5.86	5.71	5.59	7.50	8.16	5.26	3.94	6.38
Eu (0.05)	0.70	0.81	1.10	1.09	1.11	1.22	1.58	1.55	1.56	1.71	1.60	1.16	1.19	1.28
Tb (0.2)	0.36	0.47	0.59	0.60	0.72	0.90	0.85	0.98	0.96	1.27	1.41	0.94	0.70	1.06
Ho (0.2)	0.49	0.67	0.75	0.79	0.94	1.28	1.11	1.26	1.27	1.74	2.01	1.18	0.89	1.48
Yb (0.03)	1.32	1.75	1.69	1.83	2.20	3.04	2.78	2.89	2.74	4.19	5.00	2.50	1.90	3.63
Lu (0.01)	0.20	0.25	0.24	0.26	0.32	0.43	0.41	0.41	0.39	0.59	0.70	0.35	0.25	0.50
Ta (0.5)	b.d.	b.d.	b.d.	b.d.	0.82	0.54	0.93	0.84	0.65	1.11	1.47	0.94	0.34	0.92
Hf (0.2)	1.30	1.66	2.65	2.53	4.66	3.52	6.02	5.12	4.06	7.83	9.79	4.91	2.61	6.66
Th (0.2)	1.85	1.90	5.62	3.59	11.40	6.09	14.20	8.19	6.29	13.70	17.30	*7.50*	*2.30*	*8.90*

Numbers in the brackets are lower levels of detections (LLD). Major elements are recalculated to 100% on anhydrous basis. Thorium analyses in samples KJ 5, 6, 7 (in italic) are obtained by XRF technique. The term "b.d." means below detection.

from south Danesfahan. Hereafter, they are called HTL (high titanium, lead) and LTL (low titanium, lead) series, respectively. The HTL series also show slightly lower Al_2O_3 content. The genuinity of this classification is further demonstrated by differences in REE abundances and patterns of the volcanic rocks from these two series. Two of the more primitive samples from each series (i.e., those with lower total REE contents) are selected for comparison. Normalised REE abundances of the samples from the HTL series show twice as much $(La/Yb)_N$ and $(Ce/Lu)_N$ ratios as the LTL series (Fig. 4).

Rather coherent trends on Harker diagrams (Fig. 2) indicate that fractional crystallisation has played a dominant role in the evolution of these rocks. Decreasing trends for Al_2O_3, FeO_t, MgO, and CaO with increasing silica and alkalis, in the basic-intermediate rock spectrum, suggest that fractional crystallisation has played the major role in evolution of volcanic rocks from the study area. For identifying the minerals involved in fractional crystallisation and evaluating their relative contribution, major mineral types in equilibrium with a basaltic andesite from a subduction setting were employed (run no. 85-44-4 in Grove *et al*., 2003). The arrows demonstrated in Fig. 2 indicate differentiation trends produced by fractional crystallisation of the minerals from a melt represented by sample DS1 (i.e., the most basic sample from the study area). Employing natural mineral types analysed in similar rocks from a subduction setting (e.g., Sajona *et al*., 1996) would give rise to similar results. A careful examination of the arrows shown in Fig. 2 reveals that a mineral assemblage comprising Pl+Ol+Opaque(Sp) exerts the major control on differentiation of the volcanic rocks.

Table 2. In-house standards measured by NAA and XRF techniques at Becquerel Laboratory and UNSW respectively. All numbers (including standard deviations, S.D.) are in ppm.

NAA		GIT-IWG Recommended	GIT-IWG Analysed (average)	S.D.
	La	94.6	93.8	1.5
	Ce	196	192	3.2
	Nd	87	87.7	1.6
	Sm	18.7	19	0.3
	Eu	1.15	1.13	0.02
	Tb	3.08	2.91	0.15
	Ho	4.01	4.27	0.15
	Yb	11.4	11.6	0.2
	Lu	1.63	1.66	0.03
	Ta	5.75	5.77	0.4
	Hf	22.6	22.4	0.36
	Th	22.8	22.3	0.36
XRF		MD-1 Recommended	MD-1 Analysed (average)	S.D.
	Pb	21.3	21.7	1
	Rb	255.5	254	3.9
	Sr	531.5	525	8.2
	Ba	700.3	687	14.1
	Nb	20	19.2	2.4
	Zr	363	364.6	4.7
	Yb	21.5	23.8	3.6
	Th	18.9	19.4	1.2

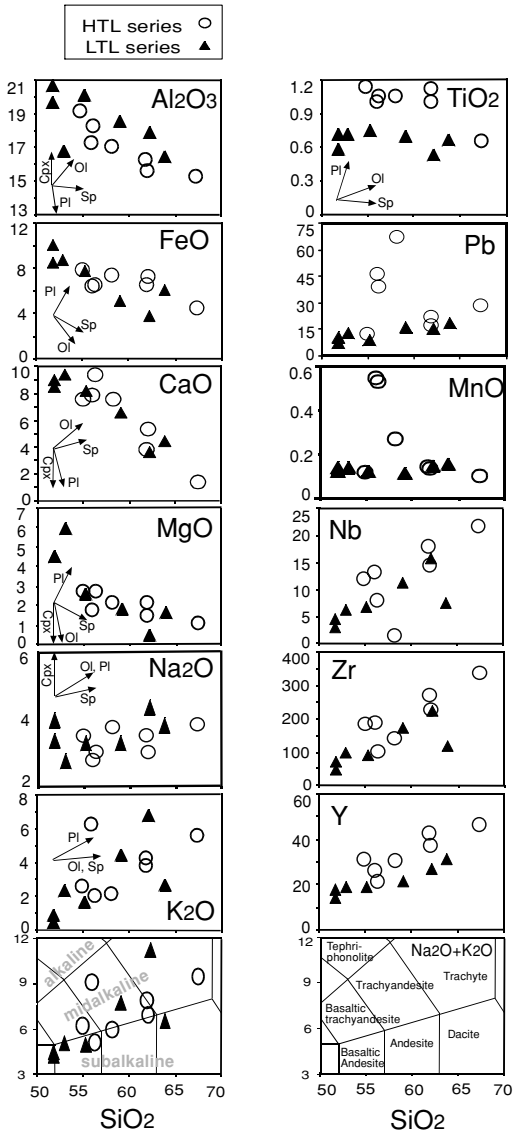

Fig. 2. SiO_2 vs. major and selected trace elements for HTL and LTL series rocks. Major element oxides are in wt.% and trace elements are in ppm. Total alkalis versus silica diagram (TAS) is after Le Bas et al., (1986) and the term 'midalkaline suite' on TAS is after Middlemost (1997). Arrows demonstrate the differentiation trends likely to develop in the volcanic rocks when fractional crystallisation (of the minerals shown) is the responsible mechanism (see text for discussion).

Abundant plagioclase phenocrysts found in the volcanic rocks confirm its role; however, altered olivine phenocrysts are rarely found, suggesting that olivine should have effectively fractionated from the magma. Clinopyroxene is a common phase both as phenocrysts and also in groundmass. Contrary to olivine that appears fractionated in the early stage of magmatic differentiation, clinopyroxene looks to be a late crystallising phase which was not fractionated to a significant extent. The fact that clinopyroxene crystals are fresh, supports their being in equilibrium with magma at the time of eruption.

Even the most basic rocks from the study area are differentiated to some extent. The highest Mg# value of these rocks is 0.48, significantly lower than those of the primary magmas (i.e., 0.69–0.76; see Jaques and Green, 1980) in equilibrium with mantle rocks. The samples are also altered to some extent, implied in part by their high L.O.I in some basic rocks (Table 1).

LTL Series; Island Arc Volcanic Rocks and Their Source Characteristics

Primitive mantle-normalised (Sun and McDonough, 1989) trace element abundances and patterns of the LTL series volcanic rocks show remarkable similarities with the calcalkaline island arc volcanic rocks (Fig. 5). These include low Nb, Ta, and Ti abundances and high ratios of LILE to LREE and HFSE (Saunders *et al*., 1980; Gill, 1981; Thompson *et al*., 1984; White and Patchett, 1984). Arc basalts are known for their low abundances of incompatible trace elements with high ionic potentials; in this respect they are even more depleted than NMORB

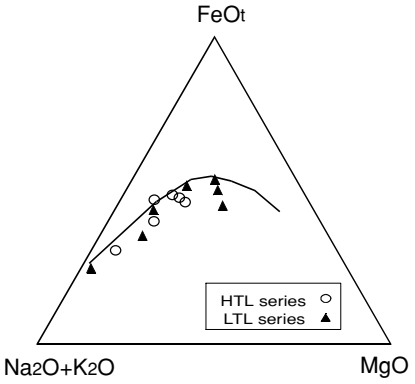

Fig. 3. Na_2O+K_2O-FeO-MgO ternary (AFM) diagram for distinction of calcalkaline from tholeiitic affinities of magmatic rocks. The boundary is from Kuno (1968).

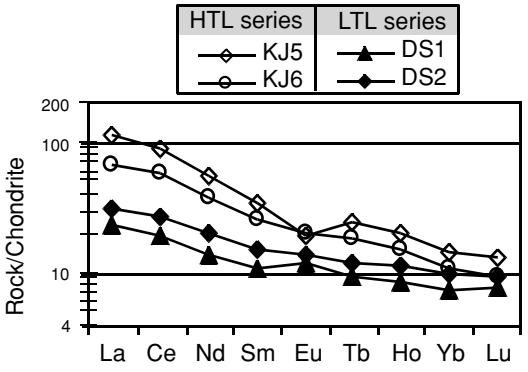

Fig. 4. Chondrite-normalised (Sun and McDonough, 1989) trace element patterns for representative basic volcanic rocks from HTL and LTL series.

(BVSP, 1981; Pearce, 1982). MORB-normalised abundances of <1 for these incompatible trace elements are noteworthy in terms of the source of island arc basalts since MORB itself is derived from a chemically depleted source (i.e., oceanic upper mantle). Usually two source components are accorded to explain the compositional characteristics of island arc basalts. One component is a Sr, Ba, and K-rich hydrous fluid or water-saturated silicate melt presumably derived from a subducting lithospheric slab. The other component is the convecting mantle wedge lying above the subducting slab. The island arc magmatism framework for the Danesfahan-Karaj volcanic rocks is consistent with the Tertiary subduction of Neotethyan oceanic slab under Central Iranian Plate.

Having emphasised its lower abundances in the LTL series as compared with the HTL series, Pb content is high enough in the former to be included in arc-related volcanics based on a Ce/Pb vs. Ce plot (Fig. 6). Due to

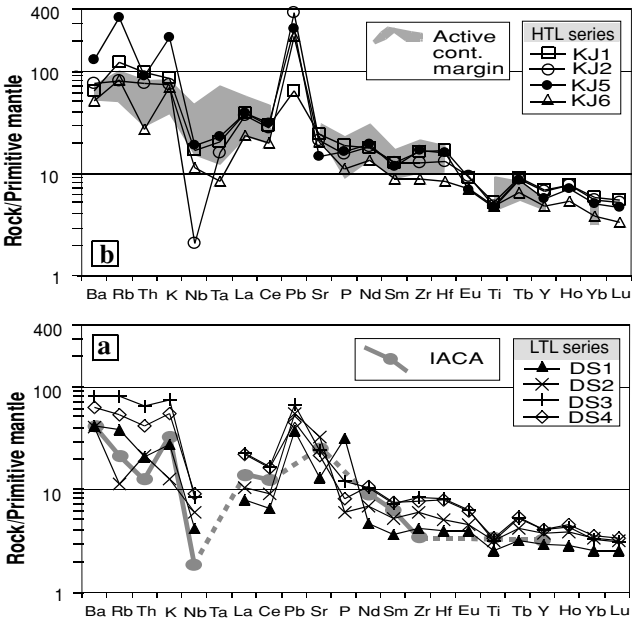

Fig. 5. Primitive mantle-normalised (Sun and McDonough, 1989) trace element patterns for basaltic-andesitic volcanic rocks from HTL and LTL series. For comparison, the typical trace element pattern of 'island arc calcalkaline basalt' (IACA: Sun, 1980) is demonstrated on diagram (a). The stippled area on diagram (b) is the combined trace element pattern of three basic rocks from northern, central and southern Andean active continental margin (Thorpe et al., 1984).

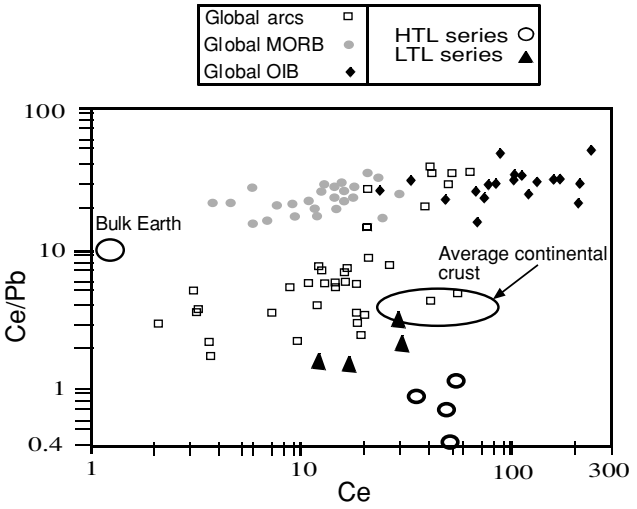

Fig. 6. Ce/Pb versus Pb diagram for basaltic-andesitic volcanic rocks from HTL and LTL series. For bulk Earth, Global arcs and Global MORB see 'figure 1' in Miller et al. (1994) and the references therein. For 'average continental crust' see 'figure 1a' in Sims and DePaolo (1997) and the references therein. The trace element data are in ppm.

similar bulk solid/liquid partition coefficients of Ce and Pb during mantle melting processes, they are not significantly fractionated during mantle melting processes, and melt compositions indicate the Ce/Pb ratio of their source region (Hofmann *et al.*, 1986). Pb is a highly incompatible element which is being concentrated in the slab-derived fluid in the course of subduction (Wilson, 1989).

HTL Series; Pb-enrichment Source and Its Characteristics

Distinguishing feature of the HTL series volcanic rocks is their high Pb contents, one of the highest ever reported in volcanic rocks. A few processes could account for such high Pb abundances.

Table 3. Partial melting trace element modeling reveals the proportion of fluid-mobile trace element, Pb, contributed by the slab. Mantle mode, melt mode, and mineral partition coefficients for Zr, Sm and Nd are adopted from Johnson (1998). Ol and Cpx partition coefficients for Pb are obtained from Hofmann and White (1983) and Halliday et al. (1995) while, for Opx it is taken from Fitton and Dunlop (1985). Sp partition coefficient for Pb is not available in the literature possibly due to both the large ionic radii of lead compared to the size of spaces avilable in Sp crystalline structure and low concentration of lead in the mantle. However, a maximum value of 0.005 is assumed for Sp partition coefficient for Pb.

Sp peridotite	Mode	Melt mode		$D_{ol/Liq}$	$D_{Opx/Liq}$	$D_{Cpx/Liq}$	$D_{Sp/Liq}$
Ol	0.53	–0.06	Zr	0.0005	0.014	0.119	0.07
Opx	0.27	0.28	Nd	0.00007	0.009	0.178	0.0006
Cpx	0.17	0.67	Sm	0.0007	0.02	0.293	0.0006
Sp	0.03	0.11	Pb	0.0003	0.0014	0.0075	0.005

	D_O	P	C_O	C HTL series			C LTL series		
				KJ2	KJ5	KJ6	DS2	DS3	DS4
Zr	0.0264	0.0913	11.2	142.5	186.7	100.1	69.9	96.6	91.0
Nd	0.0327	0.1218	1.4	24.7	26.2	18.2	9.6	14.8	15.0
Sm	0.0556	0.2019	0.4	5.6	5.3	3.9	2.4	3.4	3.5
Pb	0.0020	0.0059	0.5	67.0	46.3	38.9	10.5	6.0	8.6

Step 1. Calculating F						
	HTL series			LTL series		
	KJ2	KJ5	KJ6	DS2	DS3	DS4
Zr	0.06	0.04	0.09	0.15	0.10	0.11
Nd	0.03	0.02	0.05	0.12	0.07	0.07
Sm	0.03	0.04	0.07	0.16	0.10	0.09

Step 2. Calculating mantle-derived Pb (ppm)						
	HTL series (assuming F = 5%)			LTL series (assuming F = 10%)		
	KJ2	KJ5	KJ6	DS2	DS3	DS4
Pb	9.5	9.5	9.5	4.9	4.9	4.9

Step 3. Calculating slab-derived Pb (%)						
	HTL series			LTL series		
	KJ2	KJ5	KJ6	DS2	DS3	DS4
Pb	86	79	76	53	18	43

Enriched mantle partial melting

The involvement of an enriched (plume) mantle is a potential cause of Pb-enrichment in the volcanic rocks. Compared to the normal mantle (McKenzie and O'Nions, 1995; Tatsumi and Kogiso, 1997), enriched mantle (Fraser *et al*., 1986; McCulloch *et al*., 1983, Nelson *et al*., 1986) shows much higher Pb abundances, 0.05–1.4 ppm and 41–48 ppm, respectively. Enriched mantle seems, however, unlikely to have contributed to the high Pb content of HTL series rocks, since the HTL lack the geochemical signature of enriched mantle such as Nb-Ta peak on normalised trace element patterns. Furthermore, enriched mantle magmatism such as carbonatitic or lamproitic materials does not accompany HTL series volcanic rocks.

Higher fluid flux derived from subducted sediments

As noted above, the LTL series rocks show LILE-en-

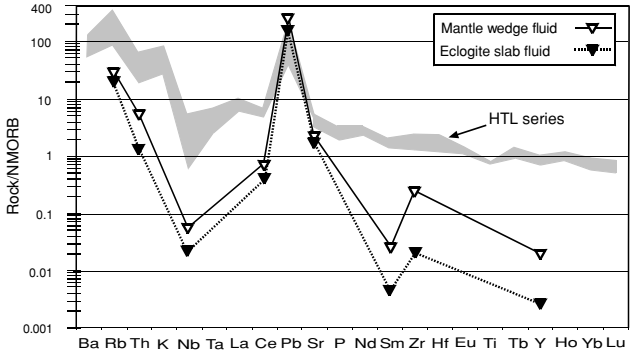

Fig. 7. NMORB-normalised (Sun and McDonough, 1989) trace element patterns for basaltic-andesitic volcanic rocks from HTL series are compared with trace element patterns of eclogite slab-derived fluids and mantle (garnet peridotite) wedge-derived fluids (Ayers, 1998).

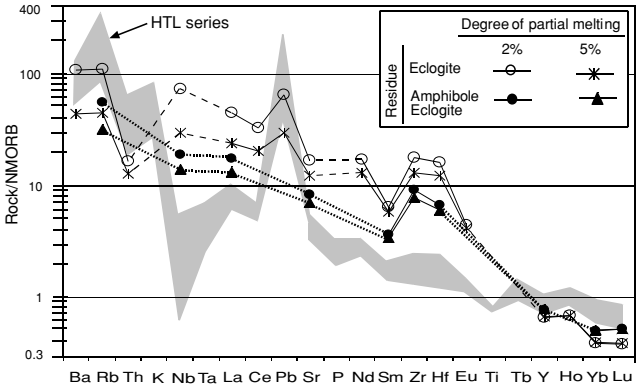

Fig. 8. NMORB-normalised (Sun and McDonough, 1989) trace element patterns for basaltic-andesitic volcanic rocks from HTL series are compared with trace element patterns of eclogite slab partial melts and amphibole-eclogite slab partial melts. See Table 3 for details.

Table 4. Trace element models of melting for NMORB. NMORB composition is taken from Hofmann (1988). Melting model assumes batch melting and "F" represents the degree of melting. Partition coefficients forCpx and Gar are after Green et al. (2000) except for Rb, Pb and Th which are taken from Halliday et al. (1995). Partition coefficients for Amph are after Green (1994) except for La, Sm and Yb which are taken from Nicholls and Harris (1980).

Element	Melting model				Melt compositions (NMORB melt)			
	NMORB	DCpx	DGar	DAmph	Cpx(50%) and Gar(50%) (Eclogite) in the residue		Cpx(35%), Gar(35%) and Amph(30%) (Amph. Eclogite) in the residue	
					F = 0.02	F = 0.05	F = 0.02	F = 0.05
Ba	13.87	0.0003	7.E-05		687.3	276.4		
Rb	1.262	0.0004	2.E-04	0.07	62.2	25.1	30.9	18.0
Th	0.1871	0.15	2.E-03		2.0	1.5		
Nb	3.507	0.00054	6.E-04	0.2	170.7	69.4	44.3	32.7
La	3.895	1.E-03	2.9E-02	0.2	111.6	60.4	43.7	33.3
Ce	12.001	3.E-03	5.5E-02		248.1	154.8		
Pb	0.489	3.E-03	8.E-03		19.4	8.9		
Sr	113.2	2.E-03	0.11	0.32	1508.8	1095.4	741.8	634.0
Nd	11.179	3.E-03	0.14		124.1	94.8		
Sm	3.752	0.18	0.23	0.8	17.0	15.3	9.5	9.1
Zr	104.24	0.12	4.3E-04	0.32	1319.3	972.3	670.8	575.1
Hf	2.974	0.07	7.3E-02	0.5	33.0	25.2	13.8	12.4
Eu	1.335	0.33	0.23		4.5	4.2		
Y	35.82	3.9	2.4E-02	1	18.4	18.7	21.6	21.8
Ho	1.342	3.7	0.25		0.7	0.7		
Yb	3.9	6.5	0.22	0.8	1.2	1.2	1.5	1.6
Lu	0.589	6.7	0.18	0.44	0.2	0.2	0.2	0.2

richment typical of island arc volcanic rocks. One might consider the HTL series volcanic rocks as being the product of similar magmatism that produced LTL series with the only difference that the former has undergone a higher degree of crustal contamination than the latter. The Carpathian volcanic arc could be cited as an example (Seghedi *et al*., 2001). The outer part of the Carpathian volcanic arc is more enriched in LILE and particularly Pb (up to 37 ppm) compared to the inner part of the arc. Therefore one can conclude that the outer part of the arc has undergone a higher degree of fluid flux than the inner part. However, compared to the LTL series, HTL series rocks are not only enriched in Pb and other LILE, but also in HFSE. Contamination by fluids derived from subducted sediments is not expected to increase the abundances of such incompatible trace elements as HFSE (e.g., Zr and Nb), since these elements are relatively immobile under hydrothermal conditions (Thirlwall *et al*., 1994; Davidson, 1996). Other processes are likely to have contributed to the higher HFSE content of HTL series: one is the lower degree partial melting in its mantle source and the other is the rather enriched nature of its mantle source. Higher Ti and Nb contents of HTL series volcanic rocks are the likely indicators of "lower degree partial melting" and "enriched mantle source", respectively. Grove *et al*. (2002) believe that TiO_2 abundances in a lava are not contributed by a fluid and may be used to estimate the fraction of silicate melting. According to Baker and Stolper (1994) Ti behaves incompatibly so it concentrates in near solidus parental melts of peridotite. The highly incompatible element Nb which is considered as an extremely sensitive trace element to depletion events (Munker, 2000), shows higher abundances in HTL series. This is an indication of the rather enriched nature of the HTL series mantle source. Reiners *et al*. (2000) pointed out that low degree partial melting of a cold rather enriched peridotite and concurrent high fluid contribution from a subducting slab are responsible for such atypical signatures (i.e., high LILE and rather high HFSE abundances) observed in HTL series volcanic rocks.

The amount of fluid-mobile trace element, Pb, contributed by the slab-derived fluid is calculated quantitatively (Table 3). The modeling entails 3 steps as follows. 1- Assuming that fluid-immobile trace elements, HFSE (e.g., Zr) and REE (e.g., Sm and Nd)) are totally contributed by mantle wedge, the degree of mantle partial melting can be calculated, 2- Using the calculated degree of mantle wedge partial melting, it is now possible to calculate the amount of fluid-mobile trace element, Pb, contributed by the mantle, and 3- Where "*a*" is the quantity of Pb contributed by the mantle wedge (obtained in step 2) and "*b*" is the total amount of Pb in the volcanic rocks, [1 – (*a*/*b*)] represents the amount of fluid-mobile trace element, Pb, contributed by the slab-derived fluid.

Nonmodal batch partial melting model is employed. The model is discussed in Wilson (1989) and represented by equation:

$$\frac{C_L}{C_O} = \frac{1}{D_O + F(1-P)}$$

in which C_L and C_O are the concentrations of a trace element in the liquid (i.e., partial melt) and original solid (i.e., mantle rock), respectively. In the equation, D_O represents bulk distribution coefficient for original solid and P is the bulk distribution coefficient for "a combination of phases entering the melt". F is the degree of partial melting. The mode of the rather fertile mantle used and the proportion of minerals involved in partial melting are adopted from Johnson (1998). The latter is consistent with experimental studies on mantle rocks partial melting (Pickering-Witter and Johnston, 2000). Details of the trace element modeling for selected basic rocks from HTL and LTL series indicate that they are produced by 2–7% (avg. = 5%) and 7–16% (avg. =10%) partial melting, respectively (step 1 in Table 3). The modeling also revealed that at least 76% of Pb in HTL series volcanic rocks is introduced by slab-derived fluid while, at most 53% of Pb in LTL series volcanic rocks is introduced by slab-derived fluid (step 3 in Table 3).

High pressure dehydration of subducted slab

Based on experimental work, Brenan *et al*. (1995) suggested that high-Pb fluids coexist with the mineral assemblage (garnet + clinopyroxene) produced by high pressure dehydration of subducted basalts. The eclogite/fluid partition coefficient for Pb is low (i.e., 0.06) since garnet strongly rejects Pb (Hauri *et al*., 1994; Halliday *et al*., 1995). These high-Pb fluids would transfer Pb to the mantle wedge overlying the subducting slab. Ayers (1998), used the modal abundances and trace element concentrations of slab eclogite and wedge lherzolite to calculate the trace element concentrations in aqueous fluids in equilibrium with these lithologies. Despite being Pb-enriched, the trace element abundances and patterns of the fluids are fundamentally different from the HTL series rocks (Fig. 7). This rules out the possibility of a major contribution by slab-derived fluids in the derivation of HTL series rocks. In other words, except for Pb, slab-derived fluid is not the main source of the HTL series rocks.

High pressure melting of subducted slab

Slab melting alone is considered the least likely model to account for island arc magmatism (Wilson, 1989). Thermal models for subduction zones imply that substantial melting of subducting oceanic crust is unlikely (Walker *et al*., 2001). However, to cover all the possibilities on

formation of the HTL series rocks, for completion it is important to now examine the likelihood of their derivation by slab melting. Assuming that a subducted slab is transferred to depths without significant geochemical alteration, we compare the geochemistry of slab partial melts with HTL series rocks. In a recent study on the geochemistry of high pressure metamorphic terrane composed of garnet blueschist to eclogite facies rocks (i.e., analogue of an oceanic crust subducted to 60 km depths) it was found that even fluid-mobile elements (i.e., LILE) may be efficiently subducted to subarc depths (Spandler *et al*., 2004). Assuming NMORB trace element chemistry for a subducting slab and the mineralogy of an eclogite and an amphibole-eclogite residues, trace element compositions of partial melts are calculated (Table 4). Compared to eclogite partial melt, partial melt compositions derived from amphibole eclogite are more akin to the HTL series volcanics (Fig. 8). By adding more amphibole to the residue, the melt would further approach the trace element configuration of HTL series rocks. However, such melts in equilibrium with substantial amount of amphibole in the residue would be felsic (Rapp and Watson, 1995) and lack the major element composition of HTL series rocks.

Tectonomagmatic framework of volcanism

The presence of Eocene island arc volcanic rocks in the study area (i.e., LTL series rocks) has not yet been explained in the context of present tectonomagmatic models (see below). Island arc magmatism requires the presence of an oceanic plate (i.e., Neotethyan Ocean) overlying a mantle wedge at the time of volcanic eruption. Earth scientists are divided on the issue of the closure time of the Neotethyan Ocean. One group believes that this has happened in Late Cretaceous (e.g., Stocklin, 1974; Berberian and King, 1981) while the others consider late Paleogene coincided with the Neotethyan closure event which leads to the continent-continent collision (e.g., Haynes and McQuillan, 1974; Sengor, 1979). Clearly our finding, the presence of Neotethyan Eocene island arc volcanism, is consistent with the latter rather than the former. Berberian *et al*. (1982), based on Rb-Sr whole rock isochron method dating of the calcalkaline plutonic rocks (i.e., 24 ± 4.5 Ma) from Natanz area (also located in UDMA; Fig. 1-a), concluded that the Arabian-Central Iranian collision should have taken place during late Paleogene or early Neogene time. In fact, in the Eocene, Urumieh-Dokhtar would have been the site of island arc volcanism. This volcanic arc was then thickened by the combined effect of volcanism and plutonism which evolved it into a mature arc and was finally developed into a crustal profile while the collision process was going on.

South Danesfahan and south Karaj, our sampling sites, lie, respectively at the western and eastern ends of a 100-km long axis almost perpendicular to the subduction trend (Fig. 1). Since subduction has occurred east-northeastwardly, it is expected that the slab deepened towards south Karaj. This means that dehydration of deeper slab contributed to HTL series volcanics (south Karaj volcanics), while the dehydration that triggered magmatism of LTL series (south Danesfahan volcanics), was rooted in the shallower slab. In general, mineralogical reactions that lead to dehydration of slab, evolve as the slab descends to greater depths. However, this can not explain the differences in chemistry of HTL and LTL series volcanics. Since HTL series volcanics are the most enriched in Pb, the slab supplying their source mantle as a reservoir of LILE, should not have undergone earlier dehydration at shallower depths. So, it is assumed that the same dehydration reaction prompted partial melting in the mantle wedge of both HTL and LTL series.

Evolution of geothermal gradients governing the subducting slab might shed some light on the processes that culminated in the petrogenesis of HTL and LTL series volcanics. The subducting slab undergoes dehydration reactions when it crosses a particular thermal limit, which we term the "dehydration geotherm". The dehydration geotherm fluctuates depending on the rate of subduction. The subducting slab is colder than its surrounding environment and its descent, at a constant rate, transfers the dehydration geotherm to greater depths until a thermal equilibrium is achieved. The increase and decrease in subduction rate move the dehydration geotherm to deeper and shallower depths, respectively. It is suggested that the subducting slab had not undergone dehydration until it reached a depth corresponding to the slab underlying south Karaj. This model helps to explain the Pb-enriched nature of the HTL series volcanic rocks, because fluids were first released from the slab underlying south Karaj. To explain the expansion of slab dehydration to shallower depths (i.e., expansion of magmatism from south Karaj to south Danesfahan) it is proposed that through time the "dehydration geotherm" shifted upwards due to the slowing down of the descending slab. In the other word, at the beginning the slab was subducting at a rather high rate (i.e., cold slab) that stimulated dehydration at deeper levels. Subsequently the subduction rate decreased (i.e., the slab became hot). This moved the dehydration geotherm upward and induced dehydration at shallower levels.

A deeper mantle source for HTL series is also supported by major element geochemistry. Slightly lower Al content of HTL series rocks, as compared with LTL series, might imply that its parental basic melt is rooted in a deeper peridotite. Peridotite partial melts at higher pressure, contain lower Al content at the same degree of partial melting (Hirose and Kushiro, 1993).

The high Pb content of HTL series rocks is compatible with the finding of Miller *et al*. (1994) that explains the preferential transport of Pb into arc magmas that eventually give rise to new continental crust. On the Ce/Pb vs. Ce plot (Fig. 6) data points from HTL series rocks deviate towards very low Ce/Pb ratios, extending the domain of arc-related magmatic material to a new-low Ce/Pb ratio, thereby confirming the involvement of a high-Pb, slab derived fluid in the genesis of these rocks from the study area. In fact, south Karaj volcanic rocks are likely to represent the transitional stage from an 'island arc' volcanism to an 'active continental margin' one. I note that low Ce/Pb ratios developed in HTL series rocks are a consequence of high Pb abundances that are fundamentally different from low Ce/Pb ratios reported as a consequence of low Ce abundances (e.g., Bohrson and Reid, 1997). Oceanic intraplate volcanics contaminated by sedimentary Fe-oxyhydroxides show negative Ce anomalies as well as variable REE abundances (Calvert, 1978; Hekinian *et al*., 1982). However, none of samples from the study area show such negative Ce anomalies (Figs. 4 and 5).

CONCLUSIONS

Introducing the trace element abundances and patterns of LTL series rocks for the first time, this study proves that an island arc-type magma was involved in Eocene magmatism in the study area. The major contribution of this study is, however, the introduction for the first time of a set of Pb-enriched volcanic rocks with transitional geochemical characteristics of an island arc-active continental margin melt. Low degree partial melting of a rather cold peridotite fluxed by Pb-enriched fluids emanating from deeper part of Neotethyan slab, produced magmas that evolved to HTL series rocks. A subsequent decrease in subduction rate, moved isotherms upward and triggered larger degree of partial melting at shallower depths, leading to LTL series rocks.

Acknowledgments—Reviews by Dr. Hiroshi Amakawa and two anonymous reviewers have significantly improved this manuscript. Their helpful comments are greatly appreciated. Research grant provided by Tarbiat Modares University is acknowledged. David Garnett and Helen Waldron of ANSTO and Irene Wainwright of UNSW are warmly thanked for meticulously carrying out the NAA and XRF analyses, respectively.

REFERENCES

Alavi, M. (1994) Tectonics of the Zagros orogenic belt of Iran: new data and interpretations. *Tectonophysics* **229**, 211–238.

Alavi, M. (1996) Tectonostratigraphic synthesis and structural style of the Alborz Mountain system in northen Iran. *J. Geodynamics* **21**, 1–33.

Amidi, S. M. (1984) Saveh Geological quadrangle map, scale: 1:250,000 (Map No. E.5). Geol. and Mineral Expl. Surv. Iran, Tehran, Iran.

Arculus, R. J. (2003) Use and abuse of the term calcalkaline and calcalkalic. *J. Petrol*. **44**, 929–935.

Ayers, J. (1998) Trace element modeling of aqueous fluid—peridotite interaction in the mantle wedge of subduction zones. *Contrib. Min. Petrol*. **132**, 390–404.

Baker, M. B. and Stolper, E. M. (1994) Determining the composition of high-pressure mantle melts using diamond aggregates. *Geochim. Cosmochim. Acta* **58**, 2811–2827.

Basaltic Volcanism Study Project (BVSP) (1981) *Basaltic Volcanism on the Terresterial Planets*. Pergamon Press, Inc., New York, 1286 pp.

Berberian, F. and Berberian, M. (1981) Tectono-plutonic episodes in Iran. *Geodynamics Series* (Delany, F. M. and Gupta, H. K., eds.), 5–32, Am. Geophys. Union.

Berberian, F., Muir, I. D., Pankhurst, R. J. and Berberian, M. (1982) Late Cretaceous and Early Miocene Andean type plutonic activity in northern Makran and Central Iran. *J. Geol. Soc. Lond*. **139**, 605–614.

Berberian, M. and King, G. C. P. (1981) Towards a paleogeography and tectonic evolution of Iran. *Can. J. Earth Sci*. **18**, 210–265.

Brenan, J. M., Shaw, H. F. and Ryerson, F. J. (1995) Experimental evidence for the origin of lead enrichment in convergent-margin magmas. *Nature* **378**, 54–56.

Calvert, S. E. (1978) Geochemistry of oceanic ferromanganese deposits. *Sea Floor Development; Moving into Deep Water* (Paton, A., Kent, P., Deacon, G., Hutchinson, K. and Ranken, M. B. F., organizers), 43–73, *Phil. Trans. Roy. Soc. Lond*. **A290**.

Davidson, J. P. (1996) Deciphering mantle and crustal signature in subduction zone magmatism. *Subduction Top to Bottom* (Bebout, G. E., Scholl, D. W., Kirby, S. H. and Platt, J. P., eds.), 251–262, *Geophys. Monogr*., Vol. 96, Am. Geophys. Union.

Dedual, E. (1967) Zur geologie des mittleren und unteren Karaj-Tales, zentral-Elburz (Iran). *Mitt. Geol. Inst. E.T.H. Univ. Zurich*, No. 79, 45–75.

Eghlimi, B., Mosavvari, F. and Mehrpartow, M. (1999) Danesfahan geological map, scale: 1:100.000 (Map No. 5961). Geol. and Mineral Expl. Surv. Iran, Tehran, Iran.

Fitton, J. G. and Dunlop, H. M. (1985) The Cameroon line, west Africa and its bearing on the origin of oceanic and continental alkali basalt. *Earth Planet. Sci. Lett*. **72**, 23–38.

Fraser, K. J., Hawkesworth, C. J., Erlang, A. J., Mitchell, R. H. and Scott-Smith, B. H. (1986) Sr, Nd and Pb isotope and minor element geochemistry of lamproites and kimberlites. *Earth Planet. Sci. Lett*. **76**, 57–70.

Gill, J. B. (1981) *Orogenic Andesites and Plate Tectonics*. Springer Verlag, Heidelberg, 390 pp.

Gordon, G. E., Randle, K., Goles, G. G., Corliss, J. B., Beson, M. H. and Oxley, S. S. (1968) Instrumental activation analysis of standard rocks with high resolution gamma-ray detectors. *Geochim. Cosmochim. Acta* **32**, 369–396.

Green, T. H. (1994) Experimental studies of trace element partitioning applicable to igneous petrogenesis—Sedona 16 years later. *Chem. Geol*. **117**, 1–36.

Green, T. H., Blundy, J. D., Adam, J. and Yaxley, G. M. (2000) SIMS determination of trace element partition coefficients between garnet, clinopyroxene, and hydrous basaltic liquids at 2–7.5 Gpa and 1080–1200°C. *Lithos* **53**, 165–187.

Grove, T. L., Parman, S. W., Bowring, S. A., Price, R. C. and Baker, M. B. (2002) The role of an H_2O-rich fluid component in the generation of primitive basaltic andesites and andesites from the Mt. Shasta region, N California. *Contrib. Min. Petrol.* **142**, 375–396.

Grove, T. L., Elkins-Tanton, L. T., Parman, S. W., Chatterjee, N., Muntener, O. and Gaetani, G. A. (2003) Fractional crystallization and mantle-melting controls on calc-alkaline differentiation trends. *Contrib. Min. Petrol.* **145**, 515–533.

Halliday, A. N., Lee, D., Tommasini, S., Davies, G. R., Paslick, C. R., Fitton, J. G. and James, D. E. (1995) Incompatible trace elements in OIB and MORB and source enrichment in the sub-oceanic mantle. *Earth Planet. Sci. Lett.* **133**, 379–395.

Hauri, E. H., Wagner, T. P. and Grove, T. L. (1994) Experimental and natural partitioning of Th, U, Pb and other trace elements between garnet, clinopyroxenes and basaltic melts. *Chem. Geol.* **117**, 149–166.

Haynes, S. J. and McQuillan, H. (1974) Evolution of the Zagros suture zone, southern Iran. *Geol. Soc. Am. Bull.* **85**, 739–744.

Hekinian, R., Renard, V. and Cheminee, J. L. (1982) Hydrothermal deposits on the East Pacific Rise near 13N: geological setting and distribution of active sulfide chimneys. *Hydrothermal Processes at Seafloor Spreading Centers* (Rona, P. A., Bostrom, K., Laubier, L. and Smith, K. L., eds.), 571–594, Plenum, New York.

Hirose, K. and Kushiro, I. (1993) Partial melting of dry peridotites at high pressures: Determination of compositions of melts segregated from peridotite using aggregates of diamond. *Earth Planet. Sci. Lett.* **114**, 477–489.

Hofmann, A. W. (1988) Chemical differentiation of the Earth: the relationship between mantle, continental crust and oceanic crust. *Earth Planet. Sci. Lett.* **90**, 297–314.

Hofmann, A. W. and White, W. M. (1983) Ba, Rb and Cs in the Earth's mantle. *Z. Naturforsch.* **38a**, 256–266.

Hofmann, A. W., Jochum, K. P., Seufert, M. and White, W. M. (1986) Nb and Pb in oceanic basalts: new constraints on mantle evolution. *Earth Planet. Sci. Lett.* **79**, 33–45.

Jaques, A. L. and Green, D. H. (1980) Anhydrous melting of peridotite at 0–15 kb pressure and the genesis of tholeiitic basalts. *Contrib. Min. Petrol.* **73**, 287–310.

Johnson, K. T. M. (1998) Experimental determination of partition coefficients for rare earth and high-field-strength elements between clinopyroxenes, garnet, and basaltic melt at high pressures. *Contrib. Min. Petrol.* **133**, 60–68.

Kuno, H. (1968) Differentiation of basalt magmas. *The Poldervaart Treatise on Rocks of Basaltic Composition*, 2 (Hess, H. H. and Poldervaart, A. A., eds.), 623–688, Interscience, New York.

Le Bas, M. J., Le Maitre, R. W., Streckeisen, A. and Zanettin, B. (1986) A chemical classification of volcanic rocks based on the total alkali-silica (TAS) diagram. *J. Petrol.* **27**, 745–750.

McCulloch, M. T., Jaques, A. L., Nelson, D. R. and Lewis, J. D. (1983) Nd and Sr isotopes in lamproites and kimberlites from western Australia: an enriched mantle origin. *Nature* **302**, 400–403.

McKenzie, D. and O'Nions, R. K. (1995) The source regions of oceanic island basalts. *J. Petrol.* **36**, 133–159.

Mehdizadeh-Tehrani, S., Yousefi, M., Emami, M. H. and Navai, I. (1995) Karaj geological map, scale: 1:100.000 (Map No. 6161). Geol. and Mineral Expl. Surv. Iran, Tehran, Iran.

Meschede, M. (1986) A method of discriminating between different types of mid-ocean ridge basalts and continental tholeiites with the Nb-Zr-Y diagram. *Chem. Geol.* **56**, 207–218.

Middlemost, E. A. K. (1997) *Magmas, Rocks and Planetary Developments, a Survey of Magma/Igneous Rock System*. Addison Wesley Longman Ltd., 299 pp.

Miller, D. M., Goldstein, S. L. and Langmuir, C. H. (1994) Cerium/lead and lead isotope ratios in arc magmas and the enrichment of lead in the continents. *Nature* **368**, 514–520.

Munker, C. (2000) The isotope and trace element budget of the Cambrian Devil River arc system, New Zealand: identification of four source components. *J. Petrol.* **41**, 759–788.

Nelson, D. R., McCulloch, M. T. and Sun, S. S. (1986) The origins of ultrapotassic rocks as inferred from Sr, Nd and Pb isotopes. *Geochim. Cosmochim. Acta* **50**, 231–245.

Nicholls, I. A. and Harris, K. L. (1980) Experimental rare earth element partition coefficients for garnet, clinopyroxene and amphibole coexisting with andesitic and basaltic liquids. *Geochim. Cosmochim. Acta* **44**, 287–308.

Norrish, K. and Hutton, J. T. (1969) An accurate X-ray spectrographic method for the analysis of a wide range of geological samples. *Geochim. Cosmochim. Acta* **33**, 431–453.

Peacock, M. A. (1931) Classification of igneous rock series. *J. Geology* **39**, 54–67.

Pearce, J. A. (1982) Trace element characteristics of lavas from destructive plate boundries. *Andesites: Orogenic Andesites and Related Rocks* (Thorpe, R. S., ed.), 525–548, Wiley.

Pickering-Witter, J. and Johnston, A. D. (2000) The effect of variable bulk composition on the melting systematics of fertile peridotitic assemblages. *Contrib. Min. Petrol.* **140**, 190–211.

Rapp, R. P. and Watson, E. B. (1995) Dehydration melting of metabasalt at 8–32 kbar: implications for continental growth and crust-mantle recycling. *J. Petrol.* **36**, 891–931.

Reiners, P. W., Hammond, P. E., McKenna, J. M. and Duncan, R. A. (2000) Young basalts of the central Washington Cascades, flux melting of the mantle, and trace element signatures of primary arc magmas. *Contrib. Min. Petrol.* **138**, 249–264.

Sajona, F. G., Maury, R. C., Bellon, H., Cotten, J. and Defant, M. (1996) High field strength element enrichment of Pliocene-Pleistocene island arc basalts, Zamboanga Peninsula, western Mindanao (Philippines). *J. Petrol.* **37**, 693–726.

Saunders, A. D., Tarney, J. and Weaver S. D. (1980) Transverse geochemical variations across the Antarctic Peninsula: implications for the genesis of calc-alkaline magmas. *Earth Planet. Sci. Lett.* **46**, 344–360.

Seghedi, I., Downes, H., Pecskay, Z., Thirlwall, M. F., Szakacs, A., Prychodko, M. and Mattey, D. (2001) Magma genesis

in a subduction-related post-collisional volcanic arc segment: the Ukranian Carpathians. *Lithos* **57**, 237–262.
Sengor, A. M. C. (1979) Mid-Mesozoic closure of Permo-Triassic Tethys and its implication. *Nature* **279**, 590–593.
Sims, K. W. W. and DePaolo, D. J. (1997) Inferences about mantle magma sources from incompatible element concentration ratios in oceanic basalts. *Geochim. Cosmochim. Acta* **61**, 765–784.
Spandler, C., Hermann, J., Arculus, R. and Mavrogenes, J. (2004) Geochemical heterogeneity and element mobility in deeply subducted oceanic crust; insights from high pressure mafic rocks from New Galedonia. *Chem. Geol.* **206**, 21–42.
Stocklin, J. (1974) Possible ancient continental margin in Iran. *The Geology of Continental Margins* (Burk, C. A. and Drake, C. L., eds.), 873–887, Springer, New York.
Stocklin, J. and Setudehnia, A. (1971) *Stratigraphic Lexion of Iran*. Geol. and Mineral Expl. Surv. Iran, Rep. No. 18, Tehran, Iran.
Sun, S. S. (1980) Lead isotopic study of young volcanic rocks from mid-ocean ridges, ocean islands and, island arcs. *Phil. Trans. Roy. Soc. Lond.* **A297**, 409–445.
Sun, S. S. and McDonough, W. F. (1989) Chemical and isotopic systematics of oceanic basalts: implications for mantle composition and processes. *Magmatism in the Ocean Basins* (Saunders, A. D. and Norry, M. J., eds.), 313–345, Geol. Soc. Spec. Publ. No. 42.
Tatsumi, Y. and Kogiso, T. (1997) Trace element transport during dehydration processes in the subducted oceanic crust: 2. Origin of chemical and physical characteristics in arc magmatism. *Earth Planet. Sci. Lett.* **148**, 207–221.
Thirlwall, M. F., Smith, T. E., Graham, A. M., Theodorou, N., Hollings, J. P., Davidson, J. P. and Arculus, R. J. (1994) High field strength element anomalies in arc lavas: source or process? *J. Petrol.* **35**, 819–838.
Thompson, R. N., Morrison, M. A., Hendry, G. I. and Parry, S. J. (1984) An assessment of the relative roles of crust and mantle in magma genesis: an elemental approach. *Phil. Trans. Roy. Soc. Lond.* **A310**, 549–590.
Thorpe, R. S., Francis, P. W. and O'Callaghan, L. (1984) Relative roles of source composition, fractional crystallisation and crustal contamination in the petrogenesis of Andean volcanic rocks. *Phil. Trans. Roy. Soc. Lond.* **A310**, 675–692.
Walker, J. A., Patino, L. C., Carr, M. J. and Feigenson, M. D. (2001) Slab control over HFSE depletions in central Nicaragua. *Earth Planet. Sci. Lett.* **192**, 533–543.
White, W. M. and Patchett, J. (1984) Hf-Nd-Sr isotopes and incompatible element abundances in island arcs: implications for magma origins and crust-mantle evolution. *Earth Planet. Sci. Lett.* **67**, 167–185.
Wilson, M. (1989) *Igneous Petrogenesis; a Global Tectonic Approach*. Chapman & Hall, 466 pp.

APPENDIX

Figure A1 shows different parts of the Saveh quadrangle (see Fig. 1) covered by the former studies. Examination of Harker diagrams (major element oxides vs. silica) for volcanic rocks from these studies, shown in Fig. A2, leads to the conclusion that the volcanic rocks from south Karaj and south Danesfahan show the most extreme/significant chemical differences; for instance very different K_2O and Al_2O_3 contents at the same SiO_2 contents of around 50 wt.%. It was thought that a comparative study of the volcanic rocks from these two areas would elucidate the major magmatic components and mantle rocks involved in their genesis.

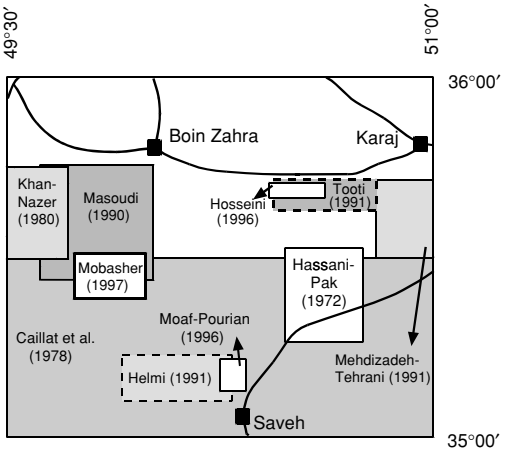

Fig. A1.

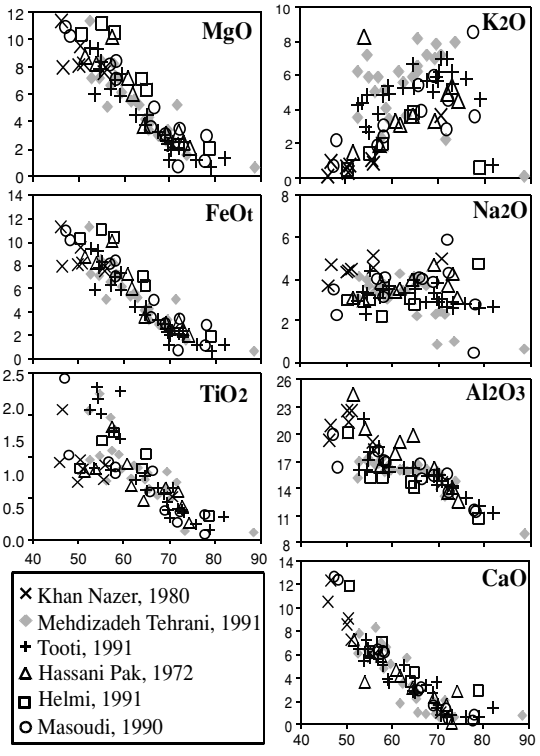

Fig. A2.